Longitudinal Alterations in the Dynamic Autoregulation of Optic Nerve Head Blood Flow Revealed in Experimental Glaucoma

Lin Wang, Grant Cull, Claude F. Burgoyne, Simon Thompson, and Brad Fortune

Devers Eye Institute, Legacy Research Institute, Portland, Oregon, United States

Correspondence: Lin Wang, Devers Eye Institute, Legacy Health, 1225 NE 2nd Avenue, Portland, OR 97232, USA;
lwang@deverseye.org.

Submitted: January 23, 2014
Accepted: April 26, 2014

Citation: Wang L, Cull G, Burgoyne CF, Thompson S, Fortune B. Longitudinal alterations in the dynamic autoregulation of optic nerve head blood flow revealed in experimental glaucoma. *Invest Ophthalmol Vis Sci*. 2014;55:3509–3516. DOI:10.1167/iovs.14-14020

Purpose. To use a novel dynamic autoregulation analysis (dAR) to test the hypothesis that the optic nerve head (ONH) blood flow (BF) autoregulation is disrupted during early stages of experimental glaucoma (EG) in nonhuman primates.

Methods. Retinal nerve fiber layer thickness (RNFLT, assessed by optical coherence tomography) and ONH BF (assessed by laser speckle imaging technique) were measured biweekly before and after unilateral laser treatment to the trabecular meshwork. Each nonhuman primate was followed until reaching either an early stage of damage (RNFLT loss $<$ 20%, $n = 6$) or moderate to advanced stages of damage (RNFLT loss $>$ 20%, $n = 9$). At each test, dAR was assessed by characterizing ONH BF changes during the first minute of rapid manometrical intraocular pressure (IOP) elevation from 10 to 40 mm Hg. The dAR analysis extracted the following parameters: baseline BF, average BF 10 seconds before IOP elevation; $BF_{\Delta max}$, maximum BF change from baseline BF; T_r, time from baseline BF to the $BF_{\Delta max}$; K_r, average descending BF rate.

Results. Mean postlaser IOP was 20.2 ± 5.9 and 12.3 ± 2.6 mm Hg in EG and control eyes, respectively ($P < 0.0001$). Compared with prelaser values, baseline BF was higher in early EG, but lower in moderate to advanced EG ($P = 0.01$). T_r was increased and K_r was reduced in both stages ($P < 0.01$). $BF_{\Delta max}$ was smaller in the early EG ($P = 0.05$) and remained low in the moderate to advanced EG ($P = 0.15$). No changes in the parameters were observed in control eyes.

Conclusions. Chronic IOP elevation causes ONH autoregulation dysfunction in the early stage of EG, characterized by a disrupted BF response and delayed T_r, revealed by dAR analysis.

Keywords: autoregulation, optic nerve head, experimental glaucoma

Autoregulation is the ability of an organ to maintain a constant local blood flow (BF) despite fluctuations in perfusion pressure. It has been proposed that autoregulation weakens or fails in glaucoma,[1–9] causing the ocular BF response to fluctuations of ocular perfusion pressure (OPP) to be more passive, rising too high when the OPP increases or dropping too low if the OPP decreases. The latter scenario has been proposed as the cause of compromised optic nerve head (ONH) BF, which has been demonstrated previously in patients with primary open-angle glaucoma.[10–21]

This hypothesis has led investigators to study the autoregulation capacity of the ONH circulation in human patients with glaucoma.[22,23] In these studies, OPP was either increased (by elevating blood pressure[23]) or reduced (by elevating intraocular pressure[22]) to challenge the ONH autoregulation system. The relative change of ONH BF before and after the OPP challenge was determined and used as a quantitative index for autoregulation capacity at the tested OPP level. However, neither of these studies detected any significant autoregulation alteration. Two factors were identified by the authors of both reports as potential explanations for their negative findings: (1) limited sensitivity of the methodology used and (2) a limited range of OPP challenge they were able to achieve within the constraints of human clinical testing. Moreover, these previous studies evaluated the BF response to OPP challenges during the steady state, minutes after the OPP challenge had elapsed, when the autoregulation process had been completed; and thus only the component of autoregulation known as static autoregulation (sAR) was studied.[24]

In a recent study conducted on nonhuman primates with unilateral experimental glaucoma (EG), we demonstrated that ONH BF is mildly increased during an early stage of EG, which then declines progressively in close correlation with the loss of retinal nerve fiber layer thickness (RNFLT).[25,26] We have also demonstrated that in a subset of these EG eyes, microsphere BF measurements were generally depressed, but in some cases elevated, in the posterior ONH (retrolaminar).[25,26] Those previous results strongly suggest that ONH BF autoregulation is disrupted in this model of EG. However, our initial evaluation of ONH BF autoregulation,[27] designed to evaluate the sAR component in the same group of EG animals by measuring the pressure–flow relationship across a broad range of OPP, showed no remarkable difference between EG and control eyes. This was surprising given our expectations of disrupted autoregulation based upon evidence from our previous studies.[25–27]

While the assessment of sAR is an important approach to investigate autoregulation in both health and disease, it

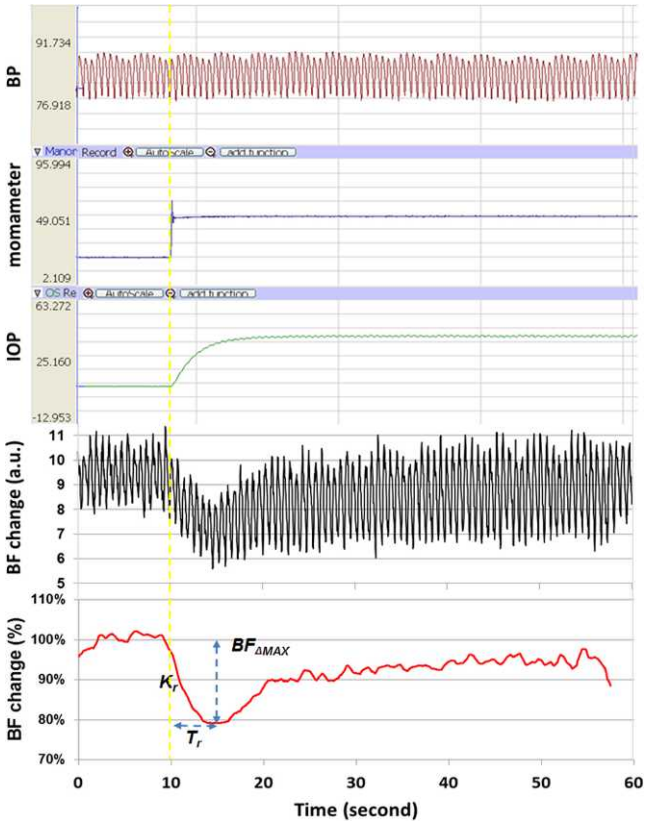

Figure 1. An example of IOP step increase-induced dAR response and parameter analysis. The *top trace* shows BP recorded 10 seconds before and during the IOP elevation. On the 10th second (*vertical yellow dotted line*), the manometer pressure (*second trace*) was rapidly increased from 10 to 40 mm Hg, resulting in a corresponding IOP increase (*third trace*). The *fourth trace* shows the LSFG recording of ONH BF response, a rapid BF decrease, and a gradual recovery toward the previous level, which took up to 3 minutes for a full recovery.[27] The bottom curve is the average from triplicate recordings of the fourth trace and smoothed (*bottom*) to remove pulsatile effects of the cardiac cycle. Four parameters were extracted to characterize the BF response curve (see text for details).

represents only the outcome of autoregulation. A different approach is to assess the complete course of BF responses during and after an OPP challenge, known as dynamic autoregulation analysis (dAR).[28–30] This approach characterizes the time course of BF responses to an acute or continuous perfusion pressure change induced artificially or spontaneously, which is a more complex but also a more accurate representation of the vascular physiology involved. Interestingly, studies in the brain have shown that these two autoregulation components, sAR and dAR, may represent different mechanisms.[31] Specifically, under certain disease conditions, impairment of the two components has been found to be disassociated,[32,33] with the dAR component likely being a more sensitive indicator than the sAR component of hemodynamic alterations in certain diseases manifesting autoregulation dysfunction.[31–33]

This analysis, developed predominantly from previous studies of cerebral and renal circulation,[29,30,34–36] has been tested for its potential application to assess autoregulation within arteries supplying the ocular vascular beds. Using rapid release of a preinflated cuff around the thighs to induce a sudden drop in systemic BP, the dAR response in the posterior ciliary arteries and central retinal artery has been characterized[37] and compared with that of the middle cerebral arteries.[38] We have also developed a time-domain analysis to quantify the dAR response within the ONH circulation by using a high spatial and temporal resolution laser speckle flowgraphy technique in conjunction with an OPP challenge elicited by acute intraocular pressure (IOP) elevation in nonhuman primates eyes.[39] Although the dAR response is slightly different when evoked by different methods and in different vascular beds, a typical dAR response to a step decrease in OPP is characterized firstly by a rapid BF decrease in the first few seconds, then a rebound, representing the rapidly changing balance of OPP and autoregulation, followed by a return of the BF toward baseline (or to a new level, see Methods and Fig. 1).

In the current study, we postulated that the sAR analysis may lack sufficient sensitivity to reveal potential autoregulation dysfunction within the ONH of human patients with glaucoma[22,23] or nonhuman primates eyes with EG.[27] Therefore, we utilized a time-domain dAR analysis previously established in our laboratory[39] to monitor the dAR response within the ONH from baseline through the moderate to advanced stage of nonhuman primate EG acquired in a previous study.[25,26] Based on the general concept of autoregulation and previous studies in the brain and other organs/tissues,[24,40,41] we predicted that the ONH dAR response would become less effective following chronic mild to moderate IOP elevation in EG eyes. Specifically, disruption of the ONH dAR response could include a faster and larger decline in BF immediately following the perfusion pressure challenge and/or delayed or incomplete rebound.

Methods

Animals

All procedures adhered to the ARVO Statement for the Use of Animals in Ophthalmic and Vision Research and were approved and monitored by the Institutional Animal Care and Use Committee (IACUC) at Legacy Research Institute. In total, 15 adult rhesus monkeys (*Macaca mulatta*) were used in the study (14 females and 1 male). Their average age (±SD) at the beginning of the study was 9.0 ± 2.6 years (range, 5–14), and average weight was 6.4 ± 1.7 kg.

Experimental Design

For each animal, three to five baseline test sessions were included to establish baseline values of IOP, RNFLT, and dAR parameters in each eye. Then chronic IOP elevation was induced by laser treatment to the trabecular meshwork in one eye of each animal. Thereafter, testing was continued every 2 weeks for the duration of the postlaser follow-up. Six animals were followed only to the early stages of EG, in which RNFLT was reduced by less than 20%. Nine animals were followed through moderate to advanced stages of damage, which was defined as RNFLT loss in the EG eye exceeding 20% of its prelaser baseline average value. The hemodynamic measurements during each postlaser stage were compared with the prelaser baseline value for each animal across the group.

Induction of Unilateral Experimental Glaucoma

Laser treatment to one eye of each animal was performed under ketamine and xylazine anesthesia. One hundred eighty degrees of the trabecular meshwork (50-μm spot size, 1.0-second duration, 600- to 750-mW power) was treated in each of two separate sessions at least 2 weeks apart. After each treatment, a sub-Tenon's injection of 0.5 mL dexamethasone (10 mg/mL) was given in the inferior fornix of the treated eye. Laser treatments were repeated (but limited to a 45°, 90°, or 180° sector) on subsequent occasions as necessary to achieve

sustained IOP elevation. The period prior to any laser treatment in the eye designated to have EG is referred to herein as the prelaser baseline, which refers to data collected in both eyes of each animal during that phase.

Testing Protocol at Each Test Session

Anesthesia. In all tests, anesthesia was induced with ketamine (15 mg/kg; Henry Schein Animal Health, Dublin, OH, USA) and xylazine (1.5 mg/kg, IM [intramuscular]; Akorn, Inc., Decatur, IL, USA), along with a single subcutaneous injection of atropine sulfate (0.05 mg/kg; Butler Schein Animal Health, Dublin, OH, USA). Animals were intubated and breathed air plus 10% oxygen. Heart rate, end-tidal CO_2, and arterial oxygenation saturation were monitored continuously. A heating pad was used to maintain the body temperature. One of the superficial branches of a tibial artery was cannulated with a 27-gauge needle, which was connected to a pressure transducer (BLPR2; World Precision Instruments, Sarasota, FL, USA) and a four-channel amplifier system (Lab-Trax-4/24T; World Precision Instruments) for continuous blood pressure (BP) recording. Anesthesia was maintained by continuous administration of pentobarbital (8–12 mg/kg/h, IV [intravenous]) using an infusion pump (Aladdin; World Precision Instruments) for all procedures except during trabecular meshwork lasering sessions. Pupils were fully dilated with 1.0% tropicamide (Alcon Laboratories, Inc., Fort Worth, TX, USA).

IOP Measurement and Manometrical Control. Intraocular pressure was measured by a rebound tonometer (Tonopen XL; Reichert, Inc., Depew, NY, USA). All IOP measurements were within 30 minutes of general anesthesia induction and represent the average of three repeated measurements. After the IOP was measured with a tonometer, two 27-gauge needles were inserted into the anterior chamber via the temporal corneoscleral limbus in a direction parallel to the iris. The needle tips were situated approximately 1 mm within the anterior chamber. One of the two needles was connected to a pressure transducer to register the IOP; the other needle was connected to either of two sterile saline reservoirs, each set at a different precalibrated height. The connection of the reservoirs to the anterior chamber was controlled by a solenoid valve (Valcor Engineering, Springfield, NJ, USA), which allows one of the reservoirs to be opened and the other closed so that the IOP can be changed from one level to the other nearly instantaneously. A computer mouse synchronized the valve control with the BF measurement program. As such, the BF measurement can start at a precisely controlled time point relative to the manometrical IOP change (see below) by a single mouse click.

RNFLT Measurement. The stage and progression of EG were monitored by measurement of the peripapillary RNFLT using a spectral-domain optical coherence tomography (SD-OCT) instrument (Spectralis; Heidelberg Engineering GmbH, Heidelberg, Germany). A single circular B-scan with 12° diameter was recorded in both eyes of each animal at each follow-up time point. Nine to sixteen individual sweeps were averaged to comprise the final B-scan recorded at each session. The automated layer segmentations by the instrument were corrected manually when the algorithm had obvious error during delineation of the RNFL inner and outer borders. The RNFLT values were extracted by custom software.[42]

ONH Blood Flow Measurement. The BF in the ONH was measured with a laser speckle flowgraph (LSFG; Softcare, Iizuka, Japan) as described previously.[26,43] In brief, a fundus camera within the LSFG device was focused on an area of 3.8 × 3 mm (width × height) centered on the ONH. After the laser is switched on ($\lambda = 830$ nm, maximum output power, 1.2 mW), a speckle pattern image is generated due to random interference of the scattered light from the illuminated tissue area. The area was continuously imaged by the LSFG and photographed with a charge-coupled device (700 × 480 pixels) at a frequency of 30 frames per second for 1 minute.

The recorded images were analyzed with offline analysis software (LSFG Analysis; Softcare). At first, the regions of interest on each image representing capillary perfusion were selected by a hand tool or by a threshold function provided by the software to eliminate the areas corresponding to large blood vessels. Within the selected area, the mean blur rate (MBR; a squared ratio of mean intensity to the standard deviation of light intensity of the image) was computed and used as a BF index. In previous studies, the MBR correlated well with capillary BF within the ONH validated by both microsphere[26] and hydrogen clearance methods.[44]

IOP-Evoked ONH dAR Response. During the test, both IOP and BP of the animals were registered continuously via the multiple-channel amplifier system. While the mean BP was stabilized between 80 and 95 mm Hg, a rapid reservoir pressure change from 10 to 40 mm Hg was completed by the synchronized reservoir controller. A corresponding IOP increase was induced, which evoked a BF response. The ONH BF measurement started 10 seconds before the onset of the IOP step increase and lasted for 60 seconds. The IOP challenge was repeated three times, and results were averaged to generate a mean ONH BF response curve (Fig. 1, bottom trace), with at least 3-minute intervals between consecutive measurements to allow the BF to return to its previous baseline BF level. The BP, IOP, and dAR recordings were exported for offline extraction of dAR parameters.

Analysis of dAR Parameters

The time-domain analysis established previously in our lab[39] was applied to extract the following defined parameters (Fig. 1, bottom) with a custom program using Microsoft Visual Basic (VBA 7.0; Microsoft Corporation, Redmond, WA, USA): baseline BF, the average BF (in arbitrary units) measured 10 seconds before IOP elevation; $BF_{\Delta max}$, the maximum BF change after IOP elevation expressed as a percentage of the baseline BF value (%); T_p, the descending time (second) from IOP change to the $BF_{\Delta max}$; K_p, the descending slope of BF change along the descending curve (%/s).

The corresponding OPP before and after the IOP increase was estimated by subtracting the IOP from the recorded mean arterial BP (diastolic pressure + 1/3 of pulse pressure) and an additional 5 mm Hg to account for the height difference between the eye and the femoral artery where BP was recorded.

Statistics

All IOP, RNFLT, and BF parameters were reported as an average ± standard deviation (SD) unless otherwise specified. The difference between group mean values for each parameter was evaluated by either Student's *t*-test if the data were normally distributed or by a nonparametric Wilcoxon test.

Results

IOP and RNFLT

Average IOP in the control eyes was 13.8 ± 2.3 mm Hg during the prelaser period and 12.3 ± 2.6 mm Hg during the postlaser period ($P > 0.05$). In the EG eyes, the average IOP was 14.1 ± 2.1 mm Hg during prelaser baseline and 20.2 ± 5.9 mm Hg postlaser ($P < 0.0001$). The peak IOP was 42.2 ± 10.2 mm Hg

Investigative Ophthalmology & Visual Science

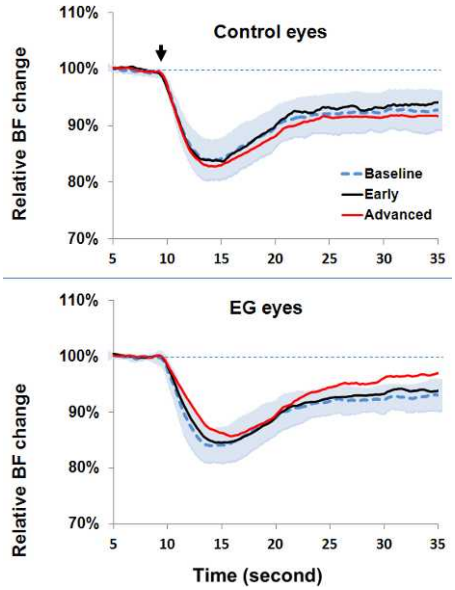

FIGURE 2. Longitudinal comparison of normalized dAR response curves between the groups of fellow control eyes (*top*) and EG eyes (*bottom*). The dAR response curves were averaged during the prelaser stage (*dotted blue curve*; the *shaded areas* represent the SD of individual animals across groups, $n = 15$ eyes), early-stage EG (*black curve*, $n = 15$ eyes), and moderate to advanced EG (*red curve*, $n = 9$ eyes) for the group of fellow control eyes (*top*) and EG eyes (*bottom*). After the IOP was acutely increased from 10 to 40 mm Hg at the 10th second (*arrow*) and continued, the BF response time (T_r) of both early- and advanced-EG eyes was significantly delayed compared with the prelaser stage. The descending slope of the BF response (K_r) was also significantly reduced. No changes were observed in the control eyes. Note that for the purposes of presentation, only a 35-second BF recording is shown.

for EG eyes and 18.9 ± 2.8 mm Hg for the control eyes. The average postlaser follow-up duration was 7.7 ± 2.6 months (range, 3.6–12.5 months). At the final test session, the average value of RNFLT in the control eyes (expressed as a percent change from the prelaser average) was –0.4 ± 2.3% (range, –6.2% to 4.3%). Final RNFLT in the EG eyes was –33 ± 22% (relative to prelaser average, $P < 0.001$). Six of the animals were followed only to a relatively early stage of EG before being humanely killed for histopathology studies. In these early-stage animals, the average RNFLT in the EG eyes was –9 ± 8% from prelaser values (range, 3.5% to –17.1%) at the final time point. Mean final RNFLT in the group of nine moderate to advanced EG eyes was –46 ± 11% from prelaser value, ranging from –36% to –62%.

Dynamic Autoregulation

As a general pattern in control eyes, the rapid IOP increase from 10 to 40 mm Hg induced an immediate ONH BF decrease (e.g., Figs. 1, 2). The BF reached a trough ($BF_{\Delta max}$) within approximately 3 to 4 seconds, typically before the IOP completely achieved its asymptotic level at the target pressure of 40 mm Hg; then BF started to rebound toward the previous level recorded with an IOP at 10 mm Hg. A full BF recovery took up to 3 minutes.

To determine the effect of experimental disease stage on the ONH dAR response, data from postlaser test sessions were grouped according to the degree of RNFLT loss in the EG eye as follows: Early-stage EG was defined as RNFLT loss less than 20% below the prelaser average; moderate- to advanced-stage EG was defined as RNFLT loss more than 20% below the prelaser average. For each of the four dAR parameters, the postlaser average value from eyes during a given EG stage was compared with the prelaser average (by two-tailed paired Student's *t*-test) for both EG eyes and fellow control eyes. This analysis was done first using postlaser data limited to early-stage EG ($n = 15$ pairs of eyes) and then repeated using only data from moderate to advanced EG ($n = 9$ pairs of eyes). Figure 3 presents the results of this analysis.

The results in Figure 3 show that three out of the four dAR parameters (baseline BF, T_r, and K_r) changed significantly from the prelaser stage in EG eyes, in both the early and moderate to advanced EG eyes, whereas there were no changes observed for dAR parameters in the fellow control eyes. Consistent with earlier observations based on previous analyses of ONH BF,[25] baseline BF was higher than at the prelaser stage in EG eyes during early EG, but lower than at the prelaser stage during moderate to advanced EG ($P = 0.01$ each). The dAR parameter T_r was increased and the dAR parameter K_r reduced in EG eyes during both early and moderate to advanced EG ($P < 0.01$ each). The dAR parameter $BF_{\Delta max}$ was smaller than prelaser values in the EG eyes during early EG ($P = 0.05$) and remained below prelaser values in moderate to advanced EG (though the latter did not achieve statistical significance, $P = 0.15$).

Mean arterial BP at the time when the dAR response was measured was 90 ± 4.8 and 88 ± 7.5 mm Hg in the early and moderate to advanced EG animals, respectively. While each value was slightly higher than the mean prelaser BP (87 ± 6.0 mm Hg), neither achieved statistical significance ($P = 0.06$ and $P = 0.09$, respectively).

DISCUSSION

In our recent studies on nonhuman primates with EG, we demonstrated that ONH BF is mildly increased during an early stage and then decreases progressively through moderate to advanced stages.[25,26] Optic nerve head BF autoregulation capacity during the corresponding stages was quantified by sAR analysis, in which we measured the BF response to an IOP challenge across a wide range of OPP after a 3-minute or greater period of stabilization. In that study, no significant difference in sAR capacity was detected between EG and fellow control eyes during any stage.[27] In the current study, we report the results of dAR analysis[39] for the same animals assessed during same stages as in the previous sAR analysis. This dAR analysis focuses on the time course of the ONH BF response within the first 60 seconds after the IOP challenge. The dAR parameters represent a dynamic balance between two forces: increased IOP, which imposes a passive vasoconstriction, and the autoregulation capacity that counteracts the effect of acutely increased IOP by dilating the blood vessels. Depending upon the relative strength of these two, the dAR parameters vary. Within the first few seconds, the effect of IOP predominates and causes a steep BF decrease at a constant rate of decline (K_r). After the initiation of autoregulation, the two effects gradually reach equivalence at a given time point (T_r), when the decline of BF ceases ($BF_{\Delta max}$) despite continued IOP elevation. The effects of normal autoregulation eventually surpass those of elevated IOP and return BF back to the baseline level observed prior to the IOP challenge in approximately 3 to 5 minutes. This latter level of stabilized BF after the end of the challenge is equivalent to the measurement of autoregulation capacity made during the sAR analysis in our previous study,[27] as well as in other studies in human glaucoma patients for other ocular vascular tissues.[22,45–47] Thus, given that autoregulation fails, we predicted that EG eyes would exhibit a steeper K_r, larger $BF_{\Delta max}$, and longer T_r, representing a less effective autoregulation capacity

Investigative Ophthalmology & Visual Science

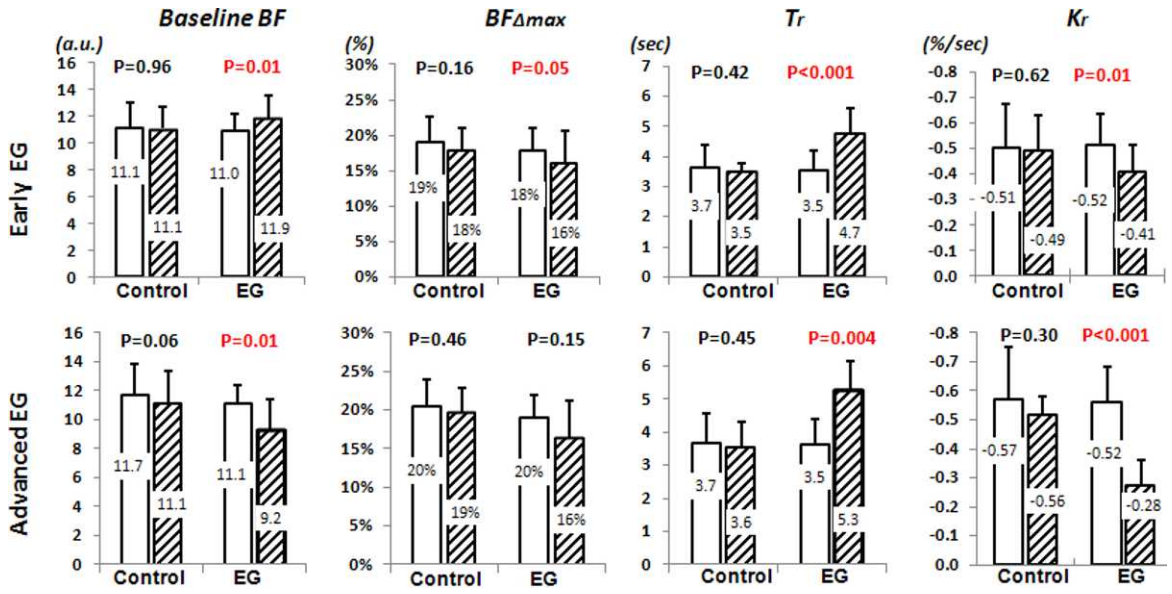

Figure 3. Comparison of dAR parameters between the prelaser stage (*unfilled bars*) and during the postlaser follow-up phase (*hatched bars*) in control eyes and EG eyes during early-stage EG ($n = 15$, *top row*) and moderate to advanced EG ($n = 9$, *bottom row*). *Each column* shows the result for one of the dAR parameters. The mean value shown by *each bar* is also listed on the bar; *error bars* represent SD. *P* values listed above each pair of bars are the result of comparing the average parameter value for a given postlaser stage against the average prelaser baseline for each individual eye across the group (two-tailed paired *t*-test).

to counteract an IOP challenge, according to the general concepts of autoregulation as demonstrated in nonocular tissues[24,40,41] and mathematical models to quantitatively define autoregulation capacity.[7,28,48]

Our results demonstrate that all dAR parameters were significantly altered in EG eyes (as compared with their prelaser measurements) with good specificity, as no such changes were observed in fellow control eyes. However, the direction of change was consistent only with the prediction for the parameter T_r, which increased above prelaser baseline in both the early and moderate to advanced stages in EG eyes. In contrast, the parameters K_r and $BF_{\Delta max}$ were both smaller than prelaser baseline in EG eyes during both early and moderate to advanced stages of EG.

Several possibilities may explain this unexpected $BF_{\Delta max}$ and K_r change. First, decreased OPP may affect the BF differently if it is induced by an increased IOP compared to that induced by a reduced BP. A recent study[49] has shown that retinal oxygen tension is less affected when the OPP is reduced by an increased IOP as compared with that achieved by decreasing BP. Second, it is likely that BF is less sensitive to an IOP increase if the vascular walls and extracellular matrix become less compliant. Previous studies have demonstrated[50,51] that the lamina and prelamina regions became thickened in early-stage EG in the nonhuman primate due to remodeling and/or de novo synthesis of connective tissues. In a separate study, the vascular walls within the center of the prelamina region were thickened with increased elastic fibers in glaucomatous human eyes.[52] It is possible that BF in the thickened blood vessels within the laminar and prelamina regions becomes more resistant to the acute IOP increase in EG eyes, resulting in a reduced $BF_{\Delta max}$ change and accordingly reduced K_r. This notion is supported by a recent study on pulsatile waveform analysis of ONH BF, in which a similar attenuated and delayed response was observed during each cardiac cycle in glaucoma patients.[53]

In contrast to the $BF_{\Delta max}$ and the K_r, the T_r increased consistently in both early and moderate to advanced stages of EG and did so independently of $BF_{\Delta max}$. Given that the slope (K_r) remains within a steady-state phase, an increased T_r would result from an increased $BF_{\Delta max}$. However, since the $BF_{\Delta max}$ and the K_r were reduced in these EG eyes, the increased T_r must be a result of an intrinsic perturbation of autoregulation. Finally, in this study, the parameter baseline BF was increased above prelaser level in early EG and reduced below prelaser level in moderate to advanced EG, which is in agreement with our previous observations in these eyes despite being based on a different measurement set.[25]

Collectively, the results presented herein and previously[25–27,54] depict a complex pattern of hemodynamic changes within the ONH after chronic IOP elevation. These changes, with significant spatial and temporal variation, manifest as a biphasic, stage-dependent change in basal BF,[25] with a varied BF response in the anterior and posterior ONH[26,54] and impaired dynamic autoregulation. Specifically, during early-stage EG, likely either due to a direct effect of elevated IOP on the blood vessels or via signals released from cells that modulate the vascular resistance, the latency of dAR increases and is accompanied by an increase in basal ONH BF, while ONH sAR is preserved. During more advanced EG, the sAR component of ONH BF autoregulation still remains similar to normal without any detectable change, but the latency of dAR increases further, and basal BF progressively declines in correlation with retinal ganglion cell axon loss (measured by RNFLT).

The altered autoregulation in the ONH of EG revealed by the dAR analysis in the current study may have important implications. First, although impaired autoregulation has been proposed as a risk factor associated with compromised ONH BF and consequent axonal damage in glaucoma, previous studies failed to show any remarkable ONH autoregulation changes based upon the sAR analysis in both EG[27] and human glaucoma.[22,23] As has been previously described, these studies used sAR analysis to assess the ocular tissue autoregulation capacity. However, once the OPP challenge begins, the BF takes minutes to stabilize. Thus, the BF is measured at different time points during the autoregulation process and may introduce larger variation. An additional limitation for the

sAR analysis is the inability to examine autoregulation within a wide OPP range due to practical considerations when such studies are carried out in a clinical setting on human subjects. Therefore, the measurement may miss a specific range of OPP within which the autoregulation capacity is diminished. Above all, the sAR analysis focuses only on the consequences of autoregulation; it overlooks the time course that may contain important, possibly earlier signs of autoregulation dysfunction. In contrast to the sAR analysis, dAR analysis avoids many of these disadvantages. The present study suggests that sAR and dAR, at least as characterized by our techniques, may represent separate components of BF autoregulation and that these components may disassociate from each other early in the disease, with the dAR component being more vulnerable than the sAR component.[32,33] A pilot study to translate the dAR analysis in human subjects to examine the ONH autoregulation is ongoing in our lab.

Second, these altered dAR parameters may reflect early signs of malfunction of ONH autoregulation. As previously mentioned, the dAR analysis reveals a balance of the forces between the imposed IOP challenge and autoregulation during the adjustment of the vascular resistance. Several cellular components have been described as playing a role during the process, including smooth muscles,[55] endothelium,[56] and pericytes.[57] Recent studies have demonstrated that astrocytes are likely involved in control of BF as well.[58,59] Interestingly, in vitro studies have demonstrated that astrocytes may induce polarized vascular responses, that is, to cause blood vessels either to constrict or dilate, depending on conditions such as the availability of nitric oxide[60] or vascular tone.[61,62] This unique feature renders astrocytes a favorable candidate as a hypothetical explanation of the surprising elevation of basal BF level during early-stage EG[25] and the unexpectedly reduced $BF_{\Delta max}$ and K_r change as demonstrated in the current study. Thus, these altered dAR parameters may represent an imperfect function of these cells, particularly astrocytes during early state of EG. Further study to test the hypothesis is ongoing in our lab.

Nevertheless, there are several limitations to the present study, which are similar to those pointed out in our previous work.[25–27] The course of EG in this model is relatively compressed compared to that seen most commonly in the human disease. Therefore, the long-term effect of elevated IOP on the autoregulation system and the pathological consequences of the autoregulation dysfunction as demonstrated in this study are unknown. Second, the primary insult of this EG model is based on increased IOP rather than a vascular disorder as has been proposed in human glaucoma.[5] Technically, the tissue volume from which the BF was measured by the LSFG was not precisely known and is subject to change during pathological conditions. There is also an inherent calibration error between in vivo and in vitro measurements[43] and limitation in tissue penetration.[63–66] Moreover, the inhibitory effect of pentobarbital on the vascular activities should also be considered,[67] although it has less of an effect on autoregulation compared with other anesthetics.[28,68–70] Therefore, the results of this EG model may not accurately predict the hemodynamic status in the human disease and should be interpreted with caution.

In summary, our study demonstrates early ONH BF autoregulation dysfunction characterized by an altered dynamic ONH BF response during IOP-induced OPP fluctuations. Although the exact role of these altered autoregulation metrics in contributing to the pathological consequences of glaucoma such as axon injury requires further investigation, this study reveals for the first time significantly altered autoregulation capacity by using dAR analysis. Given that similar ONH autoregulation changes develop in human glaucoma with increased IOP and in those whose autoregulation dysfunction may be a causative factor, the dAR analysis is an alternative approach to the classic sAR analysis to reveal early hemodynamic changes in the ONH microcirculation.

Acknowledgments

The authors thank Chelsea Piper for her technical assistance.

Supported by National Institutes of Health Grant R01-EY019939 and Legacy Good Samaritan Foundation, Portland, Oregon, United States.

Disclosure: **L. Wang**, None; **G. Cull**, None; **C.F. Burgoyne**, None; **S. Thompson**, None; **B. Fortune**, None

References

1. Maumenee AE. Causes of optic nerve damage in glaucoma. Robert N. Shaffer lecture. *Ophthalmology*. 1983;90:741–752.
2. Flammer J, Orgul S, Costa VP, et al. The impact of ocular blood flow in glaucoma. *Prog Retin Eye Res*. 2002;21:359–393.
3. Hayreh SS. The 1994 Von Sallman Lecture. The optic nerve head circulation in health and disease. *Exp Eye Res*. 1995;61:259–272.
4. Anderson DR. Introductory comments on blood flow autoregulation in the optic nerve head and vascular risk factors in glaucoma. *Surv Ophthalmol*. 1999;43(suppl 1):S5–S9.
5. Flammer J, Konieczka K, Flammer AJ. The primary vascular dysregulation syndrome: implications for eye diseases. *EPMA J*. 2013;4:14.
6. Grieshaber MC, Mozaffarieh M, Flammer J. What is the link between vascular dysregulation and glaucoma? *Surv Ophthalmol*. 2007;52(suppl 2):S144–S154.
7. Harris A. *Ocular Blood Flow in Glaucoma: Myths and Reality*. Amsterdam: Kugler Publications; 2009.
8. Pillunat LE, Stodtmeister R, Wilmanns I, Christ T. Autoregulation of ocular blood flow during changes in intraocular pressure. Preliminary results. *Graefes Arch Clin Exp Ophthalmol*. 1985;223:219–223.
9. Venkataraman ST, Flanagan JG, Hudson C. Vascular reactivity of optic nerve head and retinal blood vessels in glaucoma—a review. *Microcirculation*. 2010;17:568–581.
10. Jia YL, Morrison JC, Tokayer J, et al. Quantitative OCT angiography of optic nerve head blood flow. *Biomed Opt Express*. 2012;3:3127–3137.
11. Yokoyama Y, Aizawa N, Chiba N, et al. Significant correlations between optic nerve head microcirculation and visual field defects and nerve fiber layer loss in glaucoma patients with myopic glaucomatous disk. *Clin Ophthalmol*. 2011;5:1721–1727.
12. Sugiyama T, Shibata M, Kojima S, Ikeda T. Optic nerve head blood flow in glaucoma. In: Kubena T, ed. *Mystery of Glaucoma*. New York: InTech; 2011:207–218.
13. Chiba N, Omodaka K, Yokoyama Y, et al. Association between optic nerve blood flow and objective examinations in glaucoma patients with generalized enlargement disc type. *Clin Ophthalmol*. 2011;5:1549–1556.
14. Sato EA, Ohtake Y, Shinoda K, Mashima Y, Kimura I. Decreased blood flow at neuroretinal rim of optic nerve head corresponds with visual field deficit in eyes with normal tension glaucoma. *Graefes Arch Clin Exp Ophthalmol*. 2006;244:795–801.
15. Hafez AS, Bizzarro RL, Lesk MR. Evaluation of optic nerve head and peripapillary retinal blood flow in glaucoma patients, ocular hypertensives, and normal subjects. *Am J Ophthalmol*. 2003;136:1022–1031.
16. Piltz-seymour JR, Grunwald JE, Hariprasad SM, Dupont J. Optic nerve blood flow is diminished in eyes of primary open-angle glaucoma suspects. *Am J Ophthalmol*. 2001;132:63–69.

17. Findl O, Rainer G, Dallinger S, et al. Assessment of optic disk blood flow in patients with open-angle glaucoma. *Am J Ophthalmol*. 2000;130:589–596.
18. Kerr J, Nelson P, O'Brien C. A comparison of ocular blood flow in untreated primary open-angle glaucoma and ocular hypertension. *Am J Ophthalmol*. 1998;126:42–51.
19. Michelson G, Schmauss B, Langhans MJ, Harazny J, Groh MJ. Principle, validity, and reliability of scanning laser Doppler flowmetry. *J Glaucoma*. 1996;5:99–105.
20. Michelson G, Langhans MJ, Groh MJ. Perfusion of the juxtapapillary retina and the neuroretinal rim area in primary open angle glaucoma. *J Glaucoma*. 1996;5:91–98.
21. Hamard P, Hamard H, Dufaux J, Quesnot S. Optic nerve head blood flow using a laser Doppler velocimeter and haemorheology in primary open angle glaucoma and normal pressure glaucoma. *Br J Ophthalmol*. 1994;78:449–453.
22. Weigert G, Findl O, Luksch A, et al. Effects of moderate changes in intraocular pressure on ocular hemodynamics in patients with primary open-angle glaucoma and healthy controls. *Ophthalmology*. 2005;112:1337–1342.
23. Pournaras CJ, Riva CE, Bresson-Dumont H, De Gottrau P, Bechetoille A. Regulation of optic nerve head blood flow in normal tension glaucoma patients. *Eur J Ophthalmol*. 2004; 14:226–235.
24. Paulson OB, Strandgaard S, Edvinsson L. Cerebral autoregulation. *Cerebrovasc Brain Metab Rev*. 1990;2:161–192.
25. Cull G, Burgoyne CF, Fortune B, Wang L. Longitudinal hemodynamic changes within the optic nerve head in experimental glaucoma. *Invest Ophthalmol Vis Sci*. 2013;54: 4271–4277.
26. Wang L, Cull GA, Piper C, Burgoyne CF, Fortune B. Anterior and posterior optic nerve head blood flow in nonhuman primate experimental glaucoma model measured by laser speckle imaging technique and microsphere method. *Invest Ophthalmol Vis Sci*. 2012;53:8303–8309.
27. Wang L, Burgoyne CF, Cull GA, Thompson S, Fortune B. Static blood flow autoregulation in the optic nerve head in normal and experimental glaucoma. *Invest Ophthalmol Vis Sci*. 2014; 55:873–880.
28. Tiecks FP, Lam AM, Aaslid R, Newell DW. Comparison of static and dynamic cerebral autoregulation measurements. *Stroke*. 1995;26:1014–1019.
29. Aaslid R. Cerebral autoregulation and vasomotor reactivity. *Front Neurol Neurosci*. 2006;21:216–228.
30. Dineen NE, Brodie FG, Robinson TG, Panerai RB. Continuous estimates of dynamic cerebral autoregulation during transient hypocapnia and hypercapnia. *J Appl Physiol*. 2010;108:604–613.
31. Rosengarten B, Hecht M, Kaps M. Brain activity affects dynamic but not static autoregulation. *Exp Neurol*. 2007; 205:201–206.
32. Dawson SL, Blake MJ, Panerai RB, Potter JF. Dynamic but not static cerebral autoregulation is impaired in acute ischaemic stroke. *Cerebrovasc Dis*. 2000;10:126–132.
33. Peterson EC, Tozer K, Cohen W, Lam AM, Chesnut RM. Rethinking autoregulation in traumatic brain injury: a majority of patients with disruptive dynamic autoregulation do not respond to an elevated cerebral perfusion pressure. *Neurosurgery*. 2012;71:E560.
34. van Beek AH, Claassen JA, Rikkert MG, Jansen RW. Cerebral autoregulation: an overview of current concepts and methodology with special focus on the elderly. *J Cereb Blood Flow Metab*. 2008;28:1071–1085.
35. Panerai RB. Transcranial Doppler for evaluation of cerebral autoregulation. *Clin Auton Res*. 2009;19:197–211.
36. Panerai RB. Cerebral autoregulation: from models to clinical applications. *Cardiovasc Eng*. 2008;8:42–59.
37. Kaya S, Kolodjaschna J, Berisha F, Schmetterer L, Garhofer G. Comparison of the autoregulatory mechanisms between central retinal artery and posterior ciliary arteries after thigh cuff deflation in healthy subjects. *Microvasc Res*. 2011;82: 269–273.
38. Kolodjaschna J, Berisha F, Lung S, Schima H, Polska E, Schmetterer L. Comparison of the autoregulatory mechanisms between middle cerebral artery and ophthalmic artery after thigh cuff deflation in healthy subjects. *Invest Ophthalmol Vis Sci*. 2005;46:636–640.
39. Liang Y, Fortune B, Cull G, Cioffi GA, Wang L. Quantification of dynamic blood flow autoregulation in optic nerve head of rhesus monkeys. *Exp Eye Res*. 2010;90:203–209.
40. Vavilala MS, Lee LA, Lam AM. Cerebral blood flow and vascular physiology. *Anesthesiol Clin North America*. 2002;20:247–264.
41. Vaquero J, Chung C, Blei AT. Cerebral blood flow in acute liver failure: a finding in search of a mechanism. *Metab Brain Dis*. 2004;19:177–194.
42. Fortune B, Burgoyne CF, Cull GA, Reynaud J, Wang L. Structural and functional abnormalities of retinal ganglion cells measured in vivo at the onset of optic nerve head surface change in experimental glaucoma. *Invest Ophthalmol Vis Sci*. 2012;53:3939–3950.
43. Sugiyama T, Araie M, Riva CE, Schmetterer L, Orgul S. Use of laser speckle flowgraphy in ocular blood flow research. *Acta Ophthalmol*. 2010;88:723–729.
44. Takahashi H, Sugiyama T, Tokushige H, et al. Comparison of CCD-equipped laser speckle flowgraphy with hydrogen gas clearance method in the measurement of optic nerve head microcirculation in rabbits. *Exp Eye Res*. 2013;108:10–15.
45. Grunwald JE, Riva CE, Stone RA, Keates EU, Petrig BL. Retinal autoregulation in open-angle glaucoma. *Ophthalmology*. 1984;91:1690–1694.
46. Nagel E, Vilser W, Lanzl IM. Retinal vessel reaction to short-term IOP elevation in ocular hypertensive and glaucoma patients. *Eur J Ophthalmol*. 2001;11:338–344.
47. Feke GT, Pasquale LR. Retinal blood flow response to posture change in glaucoma patients compared with healthy subjects. *Ophthalmology*. 2008;115:246–252.
48. Harris A, Guidoboni G, Arciero JC, Amireskandari A, Tobe LA, Siesky BA. Ocular hemodynamics and glaucoma: the role of mathematical modeling. *Eur J Ophthalmol*. 2013;23:139–146.
49. Tani T, Nagaoka T, Nakabayashi S, Yoshioka T, Yoshida A. Mechanisms responsible for autoregulation of retinal blood flow in response to reductions in ocular perfusion pressure in cats. *Invest Ophthalmol Vis Sci*. 2014;55:360–367.
50. Yang H, Downs JC, Girkin C, et al. 3-D histomorphometry of the normal and early glaucomatous monkey optic nerve head: lamina cribrosa and peripapillary scleral position and thickness. *Invest Ophthalmol Vis Sci*. 2007;48:4597–4607.
51. Yang H, Thompson H, Roberts MD, Sigal IA, Downs JC, Burgoyne CF. Deformation of the early glaucomatous monkey optic nerve head connective tissue after acute IOP elevation in 3-D histomorphometric reconstructions. *Invest Ophthalmol Vis Sci*. 2011;52:345–363.
52. Tektas OY, Lutjen-Drecoll E, Scholz M. Qualitative and quantitative morphologic changes in the vasculature and extracellular matrix of the prelaminar optic nerve head in eyes with POAG. *Invest Ophthalmol Vis Sci*. 2010;51:5083–5091.
53. Shiga Y, Omodaka K, Kunikata H, et al. Waveform analysis of ocular blood flow and the early detection of normal tension glaucoma. *Invest Ophthalmol Vis Sci*. 2013;54:7699–7706.
54. Quigley HA, Hohman RM, Sanchez R, Addicks EM. Optic nerve head blood flow in chronic experimental glaucoma. *Arch Ophthalmol*. 1985;103:956–962.
55. Guyton AC, Hall JE. *Textbook of Medical Physiology*. 11th ed. Philadelphia: Elsevier, Inc.; 2006:161–257.

Investigative Ophthalmology & Visual Science

56. Haefliger IO, Meyer P, Flammer J, Luscher TF. The vascular endothelium as a regulator of the ocular circulation: a new concept in ophthalmology? *Surv Ophthalmol*. 1994;39:123–132.
57. Anderson DR, Davis EB. Glaucoma, capillaries and pericytes. 5. Preliminary evidence that carbon dioxide relaxes pericyte contractile tone. *Ophthalmologica*. 1996;210:280–284.
58. Takano T, Tian GF, Peng W, et al. Astrocyte-mediated control of cerebral blood flow. *Nat Neurosci*. 2006;9:260–267.
59. Attwell D, Buchan AM, Charpak S, Lauritzen M, Macvicar BA, Newman EA. Glial and neuronal control of brain blood flow. *Nature*. 2010;468:232–243.
60. Metea MR, Newman EA. Glial cells dilate and constrict blood vessels: a mechanism of neurovascular coupling. *J Neurosci*. 2006;26:2862–2870.
61. Blanco VM, Stern JE, Filosa JA. Tone-dependent vascular responses to astrocyte-derived signals. *Am J Physiol Heart Circ Physiol*. 2008;294:H2855–H2863.
62. Filosa JA, Iddings JA. Astrocyte regulation of cerebral vascular tone. *Am J Physiol Heart Circ Physiol*. 2013;305:H609–H619.
63. Johansson K, Ahn H, Lindhagen J, Lundgren O. Tissue penetration and measuring depth of laser Doppler flowmetry in the gastrointestinal application. *Scand J Gastroenterol*. 1987;22:1081–1088.
64. Koelle JS, Riva CE, Petrig BL, Canstoun SD. Depth of tissue sampling in the optic nerve head using laser Doppler flowmetry. *Lasers Med Sci*. 1993;8:49–54.
65. Riva CE, Harino S, Petrig BL, Shonat RD. Laser Doppler flowmetry in the optic nerve. *Exp Eye Res*. 1992;55:499–506.
66. Wang L, Cull G, Cioffi GA. Depth of penetration of scanning laser Doppler flowmetry in the primate optic nerve. *Arch Ophthalmol*. 2001;119:1810–1814.
67. Wang Z, Schuler B, Vogel O, Arras M, Vogel J. What is the optimal anesthetic protocol for measurements of cerebral autoregulation in spontaneously breathing mice? *Exp Brain Res*. 2010;207:249–258.
68. Werner C, Lu H, Engelhard K, Unbehaun N, Kochs E. Sevoflurane impairs cerebral blood flow autoregulation in rats: reversal by nonselective nitric oxide synthase inhibition. *Anesth Analg*. 2005;101:509–516.
69. Kremser PC, Gewertz BL. Effect of pentobarbital and hemorrhage on renal autoregulation. *Am J Physiol*. 1985; 249:F356–F360.
70. Preckel MP, Leftheriotis G, Ferber C, Degoute CS, Banssillon V, Saumet JL. Effect of nitric oxide blockade on the lower limit of the cortical cerebral autoregulation in pentobarbital-anaesthetized rats. *Int J Microcirc Clin Exp*. 1996;16:277–283.

Investigative Ophthalmology & Visual Science